RESEARCH PAPER

PCCP
www.rsc.org/pccp

Role of water molecules in the KcsA protein channel by molecular dynamics calculations

M. Compoint, C. Boiteux, P. Huetz, C. Ramseyer* and C. Girardet

Laboratoire de Physique Moléculaire, UMR CNRS 6624, Université de Franche-Comté, F-25030 Besançon Cedex, France. E-mail: christophe.ramseyer@univ-fcomte.fr

Received 10th June 2005, Accepted 15th September 2005
First published as an Advance Article on the web 6th October 2005

Molecular dynamics simulations supported by electrostatic calculations have been conducted on the KcsA channel to determine the role of water molecules in the pore. Starting from the X-ray structure of the KcsA channel in its closed state at 2.0 Å resolution, the opening of the pore towards a conformation built on the basis of EPR results is studied. We show that water molecules act as a structural element for the K^+ ions inside the filter and the hydrophobic cavity of the channel. In the filter, water tends to enhance the depth of the wells occupied by the K^+ ions, while in the cavity there is a strong correlation between the water molecules and the cavity ion. As a consequence, the protein remains very stable in the presence of three K^+ ions in the selectivity filter and one in the cavity. The analysis of the dynamics of water molecules in the cavity reveals preferred orientations of the dipoles along the pore axis, and a correlated behavior between this dipole orientation and the displacement of the K^+ ion during the gating process.

1. Introduction

The equilibrium and dynamical properties of a solvent in confined geometry can be very different from those in the bulk.[1–3] This is particularly important in the case of confined environments present in proteins, such as the interior of deep crevices, pockets or other poorly accessible regions. Prominent examples include the substrate binding sites of enzymes[4] and the narrow pores of membrane channels.[3] Simulation studies of a number of channel models with cylindrical shapes have suggested that the average dynamical properties of water molecules in a protein pore differ substantially from those in bulk water, exhibiting in particular decreased translational and rotational mobility.[3,5–7] Molecular dynamics (MD) has been used to simulate the behavior of water molecules located between two planar hydrophobic surfaces[8] or within cylindrical and spherical cavities.[9,10] These studies have shown that water confined in such molecular sized volumes displays a greater degree of order than in bulk, with the formation of distinct layers of molecules parallel to the surfaces. This confinement changes the dielectric constant of the solvent which, in turn, influences the effective electrostatic field within the liquid.[11] The situation becomes more complicated when we consider ionic channels since, in addition to the influence of the confinement due to the specific geometry of the polypeptide chains,[5] much larger variations of the dielectric constant are obtained due to the solvation of ions, like K^+, present in the channel.[12–14] There are few experimental measurements of the solvent dielectric constant within a protein pore. Let us cite for instance experimental studies of a water pool confined in reverse micelles and biological pores, which have revealed a substantial decrease of polarization[15,16] and a dramatic slowing of the rate of relaxation of water molecules.[17–19] The behavior of water molecules bound within a cyclodextrine cycle has also been found to be very different from that in bulk water.[20,21]

Due to these specific properties relating dielectric behavior and confinement, water is becoming more and more understood as a structuring element in proteins, and *ab initio* calculations have been used to prove this feature. Frey and Cleland [22,23] have reviewed the evidence supporting the idea that short and strong hydrogen bonds could provide at least five orders of magnitude in rate acceleration of enzymatic catalysis. Green[24] has proposed that a partially charged H_5O_2 group could strongly block a voltage-gated channel by preventing motions of transmembrane helices.

In this paper we refer to a pH-gated K^+ channel from *Streptomyces lividans*,[25–28] the KcsA channel. The past few years have witnessed the determination of the structure of several species of ion channels by X-ray diffraction[29,30] and by cryoelectron microscopy.[31,32] In particular, there has been substantial advances in the structural determination of potassium channels. Combined with a large number of numerical studies,[33–43] these structures provide an opportunity to relate atomic resolution structures (3.2 and 2.0 Å resolution for KcsA) to their various physiological functions (selectivity, gating, permeation, *etc.*).[44–46] In previous studies, we have built a model for the open and closed structures of KcsA based on the 2.0 Å resolution structure.[47–49] We have conducted MD simulations based on the idea that this channel could support several K^+ ions in its pore.[12] Based on simplified arguments, four K^+ ions were assumed to occupy the pore, being alternately separated by water molecules. Their locations were chosen to be consistent with the sites determined experimentally.[27] This so-called KWKWK...K sequence was proved to be stable over nanosecond time scales in either the closed or open state of the channel.[47,48] In this paper, we try to explain this choice in a more quantitative way by investigating the structural role of the protein and water on the K^+ ions properties. The specific dynamical behavior of water molecules in the hydrophobic cavity found in KcsA has been described for the closed conformation of the pore.[3,6,50] We have conducted similar studies and tried to elucidate the correlation between the motions of the K^+ ions located in the cavity with the orientation of the water molecule in the closed and open structures.

DOI: 10.1039/b508281a

2. Theory and methods

The complexity of ion channels is such that information extracted from computational models can greatly contribute to the refinement of our understanding of their physiological properties in the cell and *de facto* to better apprehend ion channel diseases. MD simulations on protein with explicit solvents and membranes and Brownian dynamics[33–43] based on a simplified description of the pore have been used to study ion permeation at the microscopic level. Nonetheless all these models, at any level, contain more or less severe approximations. In particular, it is well known that electrostatics plays a dominant role for the protein structure and function including transmembrane architectures. Macroscopic continuum electrostatic models, in which the solvent is described as a structureless dielectric medium, are particularly useful to reveal the dominant energetic factors related to ion permeation, but they occult the specific role of individual water molecules in confined zones. This is what we want to stress by using KcsA, which is a nice example as it exhibits different types of water pockets. In this section, we briefly describe our KcsA models for the open and closed states and the MD protocols we used. Details can be found elsewhere.[47–49]

2.1. Model construction from experiments

We have built open and closed state models of the KcsA channel on the basis of experimental results. The closed conformation of KcsA, as revealed by X-ray experiments at 100 K, is a tetramer formed by four outer helices M_1, pore helices P and inner helices M_2 (Fig. 1). Three main regions appear in this protein. The narrowest part of the pore, formed by the backbone carbonyl oxygens of the amino acid sequence TVGYG (Thr75–Val76–Gly77–Tyr78–Gly79), acts as a selectivity filter (F) for the K^+ ions. It extends over about 12 Å with a mean radius of 1.4 Å. At the membrane center, the size of the pore increases to form a 5 Å radius hydrophobic cavity (C). The gate (G), which is a thin hydrophobic region formed by the inner M_2 helix bundle, closes the channel with a zone of small radius (about 1.6 Å) on the intracellular side.

Very little is known about the open state of KcsA and the relationship between the structure and gating mechanism. Homology modeling with MthK and KvAP,[51–53] which are nicely representative of the open state of the KcsA pore conformation, could have been used as a starting basic structure. Also, direct experiments on KcsA using site-directed labeling and EPR spectroscopy allowed the visualization of the structural rearrangements of the intracellular M_2 helices in the process from closed to open state.[54–56] The crystallized structure of KcsA (1JQ2), averaged over 50 protein configurations was improved by additional energy minimization using molecular mechanics to obtain the 1JQ1 structure. Three main experimental conformations (homology based structures, 1JQ2 and 1JQ1) could thus be considered as starting structures in an optimization process to reach a stable open state for KcsA. Although none of these structures are totally resolved, 1JQ1 has been chosen as being the most representative. Moreover, the positions of several C_α atoms of M_2 helices occurring in the gate region are known in a precise way (Leu86 to Gln119 for the first monomer and their analogues in the other three monomers). We have thus built a model of the open structure combining the C_α known skeleton positions of the open structure derived from EPR experiments and the well-defined closed structure modeled on the basis of X-ray data.[49] The diameter of the narrowest part of the gate in the permeation path was estimated to be about 5 Å. Nevertheless, there is currently a controversy with respect to this value which seems, on the view of Brownian dynamics results,[57] too small to allow for fast K^+ diffusion motions comparable to experimental observations.

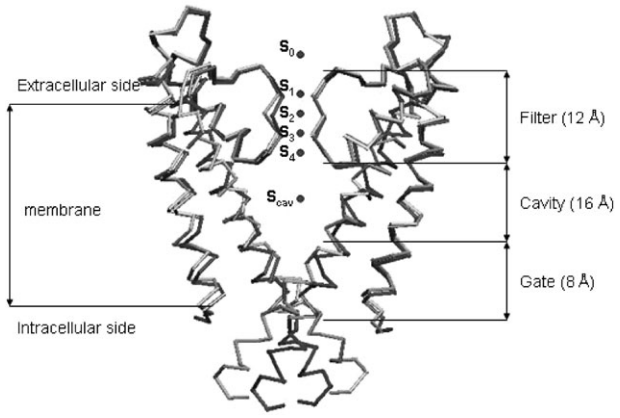

Fig. 1 Schematic representation of the KcsA channel in the closed (black) and open (grey) conformations (purple and green, respectively, in the html). For clarity, only two of the four subunits that make up the channel are shown. The 6 of 7 experimental sites for K^+ ions and water molecules are labelled S_0, S_1, S_2, S_3, S_4 and S_{cav}). The selectivity filter (F), the cavity (C) and the gate (G) are given together with their corresponding average extension.

2.2. Hydration of the different confined zones

The lipid bilayer of the cellular membrane (hydrophobic area) is mimicked by an octane box.[36,47] Of course octane molecules are not amphiphilic and cannot reproduce all the properties of a real membrane aligned phospholipids bilayer (*e.g.* different viscosity, stability, interactions with the protein) but both have nearly the same density and exhibit the same hydrophobic character. The extracellular and intracellular sides of the octane box are formed by slabs of water molecules of 22 Å thickness. We have already stressed that we must distinguish the behavior of the water molecules belonging to the intra- and extracellular areas from that of the molecules which hydrate the cavity. Therefore we fixed the density of bulk water in the extra- and intracellular sides to 1, while the density of water molecules in the cavity was determined by evaluating the Connolly surface.[58] As a consequence a bulk water molecule, which occupies on average a volume of 30 $Å^3$ at 300 K, has its mobility appreciably reduced in the cavity. This is correlated to a strong increase in water density (≥ 1). The cavity could thus contain between 30 and 40 water molecules.[35,47] The fluctuations of this number initially optimized in the closed state of KcsA were studied during the gating of the channel, in consistency with the conditions required for the hydration properties of potassium ion. Indeed MD studies using the 3.2 Å resolution structure have shown[13,42] that the K^+ ion retrieves its complete solvation shell (8 water molecules) when the cavity is filled by at least 30 water molecules.

As already mentioned, the pore axis at the filter level contains both K^+ ions and water molecules. Among the seven ionic sites observed in the 2.0 Å resolution structure[27] (2 extracellular sites S_{ext} and S_0 and 5 sites S_1 to S_{cav}) inside the channel, we deal with sites S_0 to S_{cav} because S_{ext} only appears at high K^+ concentration. Inside the filter, the filling sequence alternates, with two K^+ ions being separated by a water molecule in order to increase the solvation of the K^+ ions.[35,59] Although this quasi-linear sequence remains intuitive, its existence could be better understood by considering a steric effect (the K^+ radius and the average radius of a water molecule are close, equal to 1.33 and 1.41 Å, respectively) and the strong repulsive interaction occurring between nearest neighbor K^+ ions. On the basis of such qualitative arguments, our sequence KWKWK...K was composed of 2 water molecules (named W_1 and W_3) in the S_1 and S_3 sites and 4 potassium ions (1 extracellular, K_0, 2 ions inside the filter, K_2 and K_4, and 1

in the cavity, K_{cav}, otherwise filled by water molecules) at the S_0, S_2, S_4 and S_{cav} crystallographic sites, respectively.

2.3. MD protocols and calculated properties

The simulations were performed with the AMBER suite of programs using the AMBER6 force field.[60] The open and closed conformations were relaxed over at least 1 ns so that local minima could be ruled out.[47–49] The water molecules were described by the parameters of the TIP3P model.[61] Time steps of 1 fs were required to describe all external movements, including the water rotations. For the closed state, we have first proceeded with the solvent (water + octane) dynamics at 300 K in order to optimize the environment of the protein, the latter being frozen in its crystallized structure. In a second step, MD of the protein has been performed by increasing progressively the temperature up to 300 K during $\approx$200 ps. This simulation was continued in the (NVT) and (NPT) ensembles during 3.4 additional ns in order to follow the approach proposed by Bernèche *et al.*[35] This time was shown to be sufficient to reach equilibrium for the protein built on the basis of the 3.2 Å resolution structure.[13,42] The temperature was maintained to a constant value using Berendsen's thermal coupling[62] at 1 fs relaxation time.

Targeted MD was conducted during about 3 ns to find an open state structure of the protein.[48,49] Starting from the experimental structure 1JQ1 discussed previously, containing the KWKWK...K sequence, we progressively increased a constraint applied to each C_α atom, for reaching the open conformation.[48] This conformation was finally relaxed by releasing the constraint partially, then totally. This approach displays two main advantages over previous simulations already devoted to the gating of the KcsA channel:[39,41] (i) the refined structure of the protein contains 24 additional aminoacids at the intracellular side of the membrane, which are pointed out here as dominant for the gating mechanism; (ii) the gating mechanism is monitored step by step as a function of the constraint in an all-atom description of the pore. As shown in Fig. 1, the filter is not affected by the opening process, whereas the M_2 helices participate strongly in it. During the relaxation, the filter remains stable while M_1 and M_2 helices tend to move slightly toward closing, indicating that the pore is still significantly opened after 1.5 ns (remember that the experimental gating occurs on a millisecond time scale).

The energy profiles have been obtained by calculating the potential energy of a positive (+1e) probe charge mimicking the K^+ ion displaced adiabatically along the central (z) axis of the pore. Lennard-Jones interactions between the protein atoms, water molecules and potassium ions have also been added. Energy minimization at a given z position was made along the other directions perpendicular to the channel axis in order to follow the most favorable energetic pathway. The components of the dipole moment generated by the set of water molecules in the cavity were determined by following the orientation of all of these water molecules. The projection $\boldsymbol{\mu}_z$ of the dipole moment of each water molecule onto the z axis could then be calculated. Note that for an ideal TIP3P water molecule, the dipole moment is equal to 2.35 D.

Quantum calculations have been performed on a model of the selectivity filter containing 304 atoms.[63] We truncated the KcsA structure at the level of the four Tyr78 residues, where the peptide bond with Gly79 was cut and ended with a hydrogen (–CHO), while near the cavity below the four Thr74, –NH of the amide bond was completed in NH_2. The portion of the sequence considered was thus $(Thr74–Thr75–Val76–Gly77–Tyr78)_4$. The atomic positions were issued from MD relaxed structures. No further energy minimization was done, in order to be strictly consistent with the MD results as for the geometries. No lipidic or water environment constitutive of the MD construct was considered. We used GAUSSIAN03 suite of programs[64] to evaluate the electrostatic potential. Partial charges were fitted to reproduce the electrostatic potential surface using 6-31G(d) Hartree–Fock wave functions, with constraint of total charge conservation and following the Merz–Kollman–Singh scheme.[65,66] Determining partial charges is in general a difficult task. However, Merz–Kollman–Singh population analysis was proved to be efficient in determining such charges since it takes into account several molecular properties.[66]

3. Results and discussion

3.1. Motions of the KWKWK...K sequence

Fig. 2 shows the trajectories of the centers of mass of the K^+ ions and of the water molecules in the KWKWK...K sequence observed in the relaxed closed (Fig. 2a) and open (Fig. 2b) structures during 3.6 and 1.6 ns of the MD production run, respectively. Four main features can be extracted from these trajectories. First, the species located in the filter are strongly bound to the protein since they do not move significantly. Indeed, in the closed state, the motions of W_1, K_2, W_3 and K_4 are contained on average in spheres of diameters ranging between 2.7 and 4 Å. This behavior has been corroborated in our previous studies[47] by the calculation of the root mean square displacements (rmsd). These display very low values, from 0.5 Å in NVT conditions to 1.3 Å in NPT conditions,

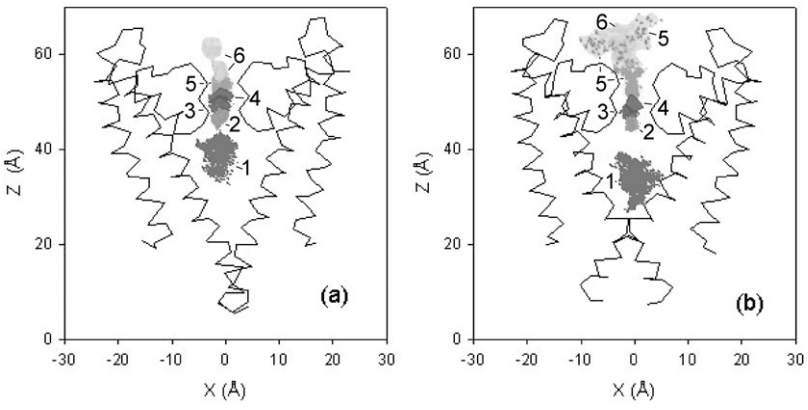

Fig. 2 Trajectories along the pore axis of the K^+ ions and water molecules in the (a) closed and (b) open conformations obtained for (a) 3.6 and (b) 1.6 ns MD runs. The various colors (in the html) determine the trajectories of the ions (K) and water molecules (W) in the filter and the cavity: K_{cav} (1, red), K_4 (2, orange), W_3 (3, blue), K_2 (4, pink), W_1 (5, green) and K_0 (6, yellow). The protein is free to rotate and translate, but for clarity we have only drawn a typical snapshot of its closed and open structures. Note that the apparent shifts of the ion trajectories in the xy plane with regard to the z axis of the protein is artificial for it is due to the superimposition of both trajectories and KcsA whose representation is a projection in the zx plane.

indicating very confined positions. Second, it should be noted that the spheres belonging to the trajectories of two adjacent species overlap. This does not mean that repulsive interactions always occur but rather shows that the atoms move in the filter in a concerted manner. Indeed, a close examination of the time dependent correlation functions of their instantaneous positions already confirmed these concerted motions within the KWKWK...K file.[47]

The third main feature concerns the K_{cav} ion, which undergoes much larger motions. In the closed state, its trajectory extends over 9.8 Å along the pore axis and 7.2 Å in the perpendicular directions. In the open state, similar trends are obtained with the respective values 11.8 Å along the pore axis and 9.1 Å in the other directions. Fourth, and perhaps most notable, the average location of the K_{cav} ion changes between the two structures. While in the closed state, this K^+ ion remains on average close to the cavity site, *i.e.* located at the upper part of the cavity as determined experimentally, but it shifts down toward the intracellular side of the cavity in the open configuration. The difference between the center of gravity of the K_{cav} trajectories in the two situations (closed and open) is equal to about 5.4 Å. Finally, let us mention that the large dispersion in the K_0 and W_1 locations observed at the outer mouth of the open structure when compared to the closed state may indicate an escape of these species from the pore.

3.2. Water as a structuring element

In this section, we analyze the structuring role of water in the filter and the cavity. Fig. 3 shows the potential energy created by the protein alone in the open and closed conformations calculated along the *z* axis by minimization of the displacement of a K^+ ion. Since the filter does not exhibit strong deformation upon gating, this energy is nearly the same in the two conformations. The curves display a deep well in the filter, with a structured shape at the well bottom, indicating the presence of sites. In the cavity and gate regions, no stable site is found for the two conformations, the main difference being obtained for the height of the barrier at the gate, which decreases by about 2 eV in the open state.

Fig. 4 exhibits the potential energy created by the filter at various *z* positions of a single K^+ ion for the closed conformation of the protein. The energy has been calculated for the protein alone with three different methods to test their accuracy. The first curve (black dots) corresponds to the potential energy extracted directly from *ab initio* calculations. The second (dark grey line, blue in the html) is calculated on the basis of the Merz–Kollman charges derived from this *ab initio* potential while the last (light grey line, red in the html) is derived directly from the AMBER force field parameters (see Fig. 3). Fig. 4 reveals that all the three methods display the same behavior, namely a deep structured well at the center of the filter. Similar depths and shapes for the wells obtained from the three methods reinforce the fact that the semi-empirical force fields used in MD simulations are reasonable enough to describe the protein environment from the point of view of the potential energy. We will therefore discuss our results on the basis of the AMBER force field, since *ab initio* calculations are in practice too time consuming for systems containing more than 300 atoms. Although the secondary minima are more or less pronounced according to the method, this comparison clearly demonstrates that the well depth is mostly due to the electrostatic interactions between the ion and the 8 carbonyl groups coming from Val55 and Gly56 in their neighboring environment. Indeed, the position of the minima correspond exactly in the three cases to the sites S_0, S_2 and S_4 determined by MD.

However it would be premature to claim at this stage that the protein field determines fully the sites and one fundamental aspect is to precisely define the influence of water. Fig. 5 exhibits the potential energy (calculated with the AMBER force field) when two water molecules W_1 and W_3 are included

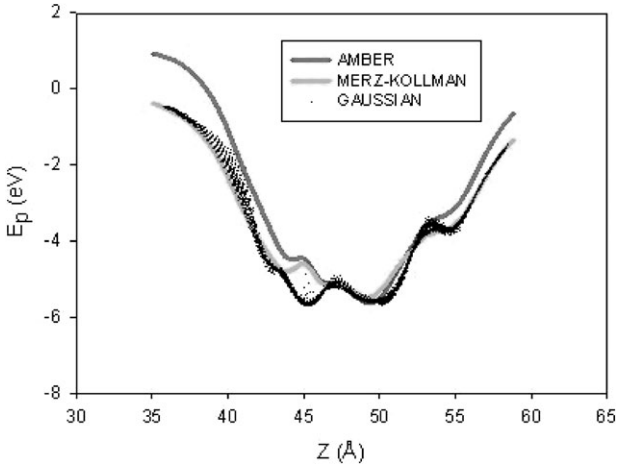

Fig. 4 Potential energy (eV) calculated for the filter alone using the *ab initio* results (black dots), Merz–Kollman charges (dark grey, blue in html) and Amber6 force field (light grey, red in html).

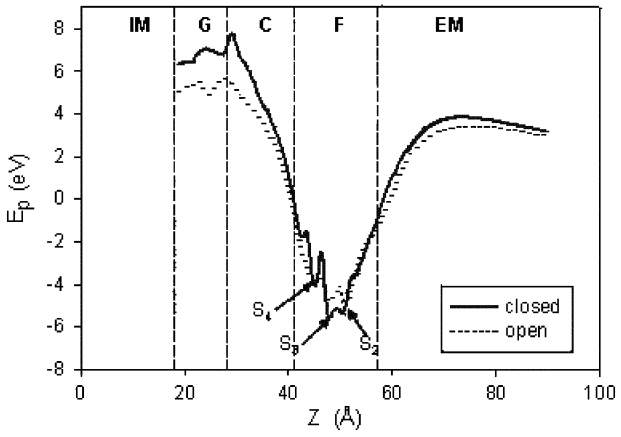

Fig. 3 Potential energy (eV) calculated with Amber force field for the protein alone in its closed (full curve) and open (dotted curve) state. The sites which are clearly prominent are given with their corresponding number.

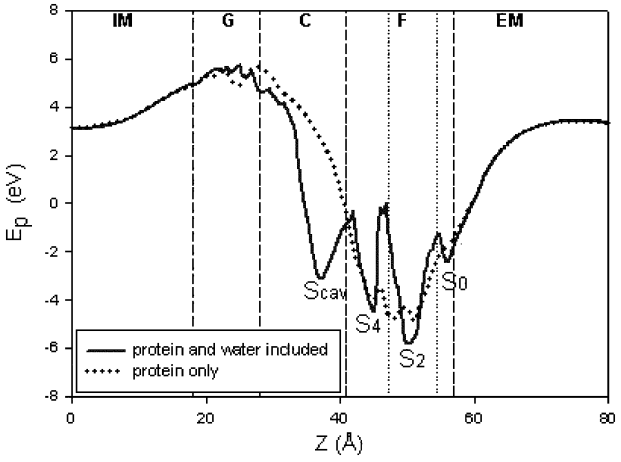

Fig. 5 Potential energy (eV) calculated using the Amber force field for the protein in its closed state with (full curve) and without (dotted curve) the presence of water molecules in the filter and cavity. The different sites are indicated.

in the filter at their preferred sites S_1 and S_3, and in addition when the cavity is hydrated. Comparison of the curves including or not the presence of water in the filter and cavity reveals its structuring role. Indeed the previous locations are clearly reinforced by the presence of the two water molecules in S_1 and S_3 since the energy experienced by the ions in sites S_2 and S_4 decreases by at least 0.5 eV. Even more indicative is the reinforcement of site S_0 as well as the occurrence of a new site corresponding exactly to the S_{cav} position. The presence of S_0 is enhanced by the W_1 water molecule. The occurrence of S_{cav} would be due to an organization of the water molecules and to the influence on the protein environment itself, both inducing the corresponding well.

As a short conclusion to this section, one can say that the water molecules in these confined positions (filter and cavity) undoubtedly play a dominant structuring role for the K^+ crossing the channel. They act first by enhancing the structure of the stable filter sites for the potassium ions, already partially outlined by the field of the protein alone, and second by revealing the cavity and S_0 sites. It should also be noted that the sites S_1 and S_3 were found stable in the closed state of the pore, on the time scale of our simulation, only if one K additional site is present in the cavity.[42]

3.3. Water as a dynamical element in the cavity

In Fig. 6, the time evolution of the components of the total dipole moment of the water molecules located in the cavity, defined as the geometrical sum of all individual H_2O dipoles, is shown for the closed and open states. A positive sign for $\boldsymbol{\mu}_z$ means that the dipole is oriented along the pore axis towards the extracellular side. This quite noisy evolution is due to several factors: the atom fluctuations in the protein, the K_{cav} motions and the thermal fluctuations in the orientational motions of light water molecules at 300 K. However, we can note that the dipoles projected along the directions perpendicular to the pore axis get close to zero on average while the component along the z axis reaches finite values. A relatively stable mean value of -10 D is obtained for the closed conformation while a $+11$ D value is reached in the open state

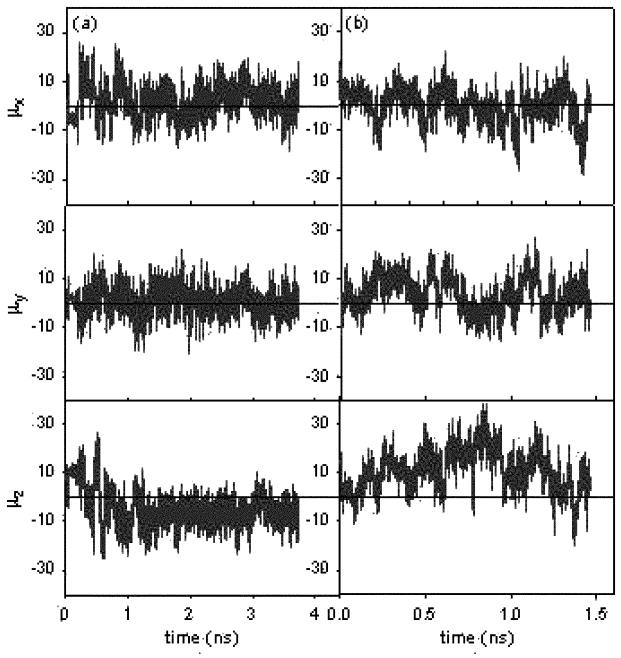

Fig. 6 Time evolution of the average dipole (Debye) of water molecules located in the cavity of the KcsA channel in its (a) closed or (b) open state. $\boldsymbol{\mu}_z$ corresponds to the dipole component along the pore axis while $\boldsymbol{\mu}_x$ and $\boldsymbol{\mu}_y$ are the components along the perpendicular directions.

with, however, much larger fluctuations and thus relatively large standard deviations from the average value. As a consequence, we expect for the open situation a large fluctuating electric field promoted by the water dipoles in the cavity.

In order to interpret these features, different hypotheses can be drawn. These finite values can be due to the dynamics of confined waters which cannot rotate freely in this hydrophobic pocket. This could also be due to the electric field created by the protein which would tend to orient the dipoles along a given direction. Finally, the field induced by the K_{cav} ion may also play an important role. Furthermore, we studied the electric field induced by the protein alone along the pore axis (not shown). This quantity can be viewed as the gradient of the potential energy discussed previously (Fig. 3). Similar behaviors are obtained for the closed and open conformations. However, a large difference occurs at the gate region where a global inversion of the electric field can be observed. Indeed for the closed structure, mainly positive values of the field indicate that K^+ ions will be pushed toward the cavity. On the contrary, K^+ ions will be pushed toward the intracellular side in the open state since the electric field exhibits mostly negative values. This feature corroborates the fact that two positions of K_{cav} are observed in the MD simulations, namely in the upper (closed state) or lower (open state) part of the cavity (Fig. 2), which is certainly also linked to the different mean orientations of the water molecule dipoles in the cavity.

A closer examination of the dynamical behavior of the water molecules leads to another interesting feature. Fig. 7 characterizes the dependence of the z component of the total dipole of water molecules in the cavity *vs.* the K_{cav} motions along the z axis of the cavity. This component $\boldsymbol{\mu}_z$ clearly follows the behavior of K_{cav}, being relatively stable when K_{cav} does not move and, on the contrary, changing its value with the ion motion. As a consequence, the orientational motions of the water molecules are more or less characterized by the ion dynamics.[42] Similar conclusions apply to the open channel with, however, larger fluctuations for K^+ displacement and water dipole component values.

To demonstrate such a correlation between the water dipole and the K_{cav} motions along the z axis, we have drawn (bottom of Fig. 7) the behavior of $\boldsymbol{\mu}_z$ *vs.* the position z of the ion center of mass in the cavity. We see three sets of points for the closed and open conformations which describe relatively well the coupled behavior $\boldsymbol{\mu}_z$ *vs.* z (K^+ position). In the closed state, the ion K_{cav} is mainly located at the upper side of the cavity around 41.5 ± 1 Å, and the corresponding dipole due to water molecules in the cavity takes values which range between 0 and -20 D, with a mean value around -10 D, as already given. The center of the cavity, around 38 ± 1 Å, is much less occupied by the K^+ ion and corresponds to a dipole ranging between -10 and $+10$ D with a vanishing mean value. The third region at the lower side of the cavity (35 ± 1 Å) is still less explored by the ion and it leads to a positive dipole whose value fluctuates significantly. In the open state, we recover the three regions, but with an occupation for the K^+ ion which is totally reversed. Indeed, the ion remains mainly located at the bottom of the cavity ($\approx$31–34 Å) and the water dipole is clearly positive. The other two regions correspond either to a K^+ location close to the center of the cavity (around 37–38 Å) or to the gate region (around 29 Å), with positive values for the water dipole, respectively small (around 0 D) and large (20–25 D), respectively. The distribution of points describing $\boldsymbol{\mu}_z$ ($z(K^+)$) displays a relatively large standard deviation, with regard to the straight lines (Fig. 7). These lines would correspond to vanishing fluctuations in the correlation between $\boldsymbol{\mu}_z$ and $z(K^+)$.

Fig. 8 shows snapshots of the pore in the closed and open states. We can see an illustrative example of what we described before. The two K^+ ions in the filter are similarly located in the two states while the K_{cav} ion occupies drastically different

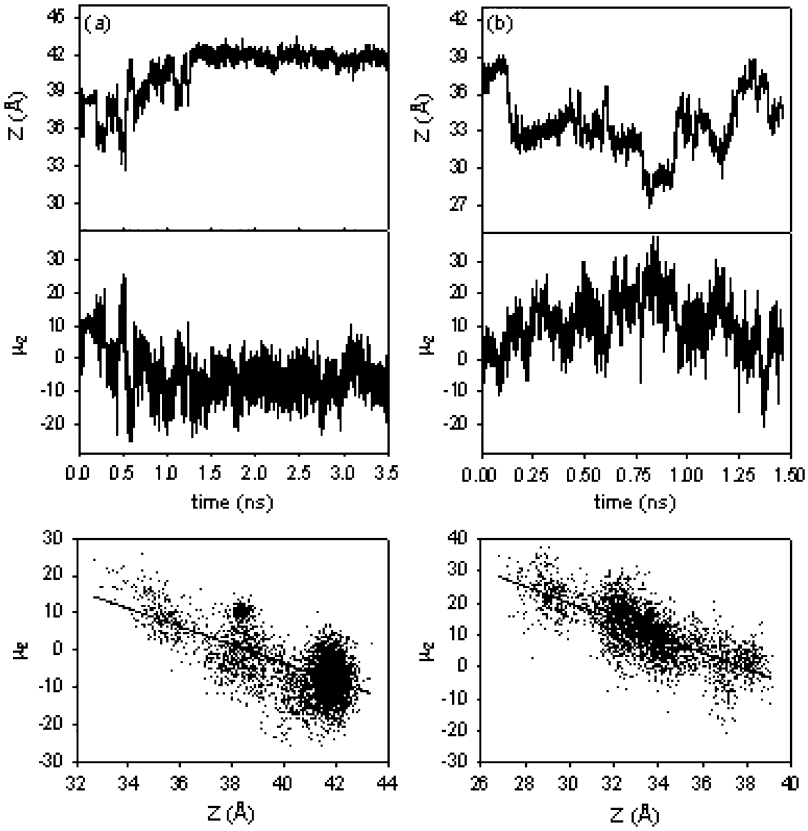

Fig. 7 Time evolution of K_{cav} positions (top) and μ_z water dipole (medium), in the (a) closed and (b) open state conformations of KcsA. μ_z *vs.* K_{cav} locations are also reported (bottom). The linear behavior of the latter curves demonstrates the fact that these two quantities evolve in a concerted manner. The deviations with respect to the linear behavior are due to large fluctuations of the water molecule orientations.

positions. A striking feature is the location of the water molecules in the cavity. In the first situation (closed state), they are all located below the ion, and thus hydrate it only partially. This means that preferential binding occurs with the innermost part of the filter, with the resulting water dipole component μ_z taking a strongly negative value (−19 D). On the contrary, in the second situation (open state), the water molecules are more equally distributed around the ion, due to the pore opening, and the corresponding dipole value becomes strongly positive (+33 D)(*i.e.* toward the extracellular side). In the open state, some water molecules are also located in the gate part, suggesting entry or exit from the cavity, while no similar behavior is observed in the closed state.

In order to study the influence of the gating mechanism, which initiates relatively large motions of the K^+ ion in the cavity, on the behavior of the water molecules motions, we have calculated (Fig. 9) the variation of the number of H_2O molecules present in the cavity. Here, we have to define the limits of the cavity. We considered that the upper side of the cavity corresponds to Thr74 while the lower side ends at the Ala108 residue. In the closed state, this number is nearly constant and equal to about 31 (not shown). The relaxation

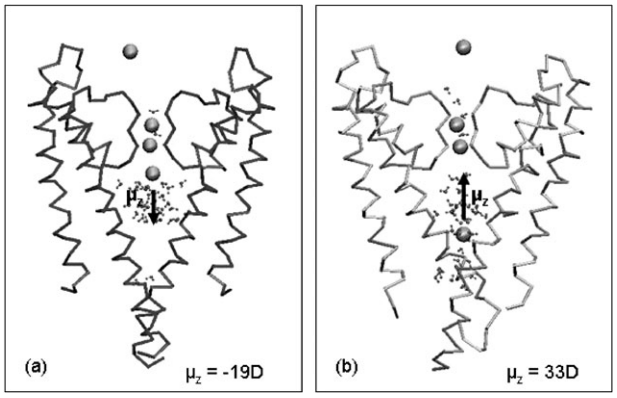

Fig. 8 Snapshots showing K^+ ions and water molecules embedded in the cavity for the (a) closed and (b) open states. For clarity, only the *xy* projected protein and water molecule location is represented. The water dipole component (D) along the pore axis is given. These two snapshots correspond to extreme situations for which (a) the K_{cav} ion is located at the mouth of the filter and partially loses its water solvation sphere (compensated by binding to the oxygen atoms of the protein wall) and (b) the ion is close to the gate and keeps its solvation sphere.

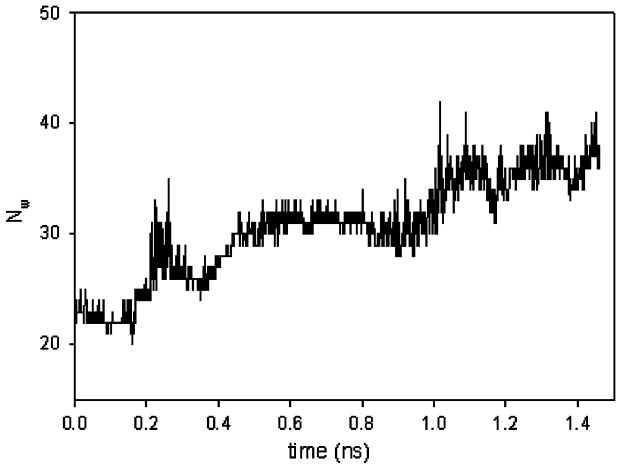

Fig. 9 Variation of the number of water molecules N_w in the cavity (see text and Fig. 10 for the definition of the limits of the cavity), as a function of the simulation time in the open state. In the first part of the curve ($t \leq 0.4$ ns), the pore relaxation induces relatively large fluctuations of N_w.

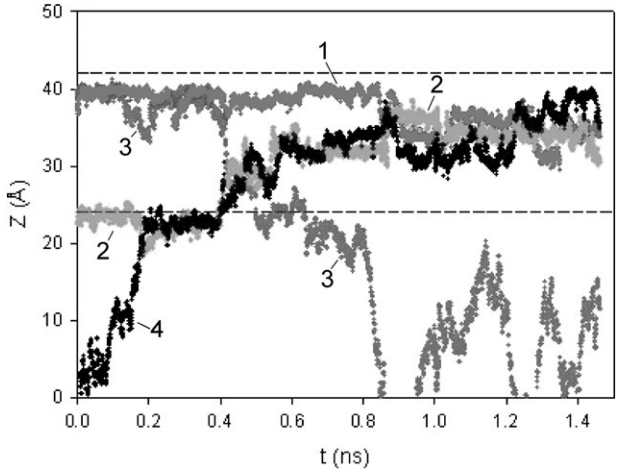

Fig. 10 Examples of water trajectories *vs.* simulation time illustrating the various situations in the cavity (the limits of the cavity are defined by broken lines): a water molecule remains inside the cavity (1, red in html), a water molecule at the gate enters and then remains in the cavity (2, green in html), a water molecule initially inside the cavity leaves and reaches the intracellular medium (3, blue in html), a water molecule initially in the intracellular region enters the cavity and remains inside it (4, black in html).

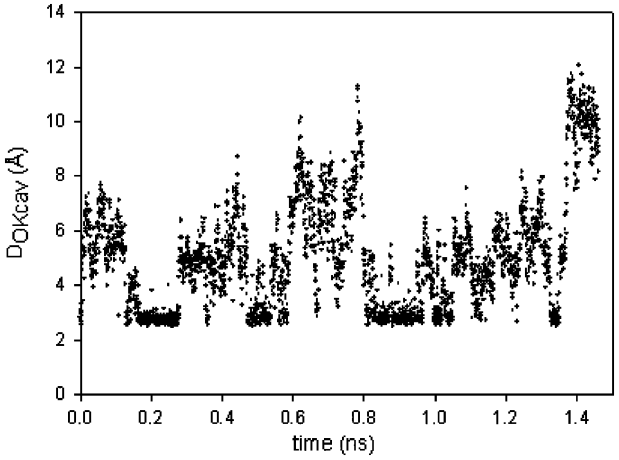

Fig. 11 Behavior of the distance D_{OK} between the centers of mass of K_{cav} and the oxygen of a water molecule *vs.* simulation time.

process which follows the constrained opening induces some perturbations at the beginning of the simulation run, resulting in a large fluctuation of the number from 22 to 30. These perturbations disappear after 0.5 ns of simulation to display a constant number of water molecules (around 32 H_2O) in the cavity. At about 1 ns, we see that the K_{cav} ion, which was located close to the gate, has moved up toward the top of the cavity (Fig. 7b), and this leads to an increase in the number of H_2O molecules (38 instead of 32). This value then fluctuates between 32 and 38, depending on the position of K_{cav} in the cavity.

Some examples of the behavior of the center of mass of some water molecules *vs.* simulation time in the open state are illustrated in Fig. 10. The first example concerns a water molecule which remains inside the cavity during the simulation time. In the second example, the molecule initially located in the gate region enters the cavity after 0.4 ns and remains confined inside. The third example corresponds to a molecule which exits the cavity after an initial $\approx$0.4 ns stay at its lower limit toward the intracellular medium. In the last example, the water molecule inside the cavity leaves. A striking behavior can be observed for all the water molecules which migrate in or outside the cavity: there is a transit residence time varying between 0.2 and 0.4 ns, *i.e.* a plateau for z *vs.* time when entering or exiting the cavity, near its lower limit. Let us mention that in the open relaxed state, among the 40 water molecules located in the filter + cavity + reservoir (on each side of KcsA), only 28 are conserved over the 1.5 ns simulation time, while 12 water molecules have been replaced by others initially located in the intracellular region. This remark shows the great mobility of water in the open pore.

Finally, it is also interesting to correlate the motions of the water molecules inside the cavity with those of K_{cav} ion. The distance between the centers of mass of the two species has been studied for most of the water molecules. In Fig. 11 we illustrate the behavior of this distance with time for one water molecule. The minimum distance $D_{OK} \approx 2.8$ Å corresponds to the radius of the first sphere of solvation for the K_{cav} ion (mean distance between the centers of mass of K^+ and oxygen atoms). We see that the water molecule spends a rather long time in this sphere, but it can also rapidly move far away from the ion, to distances that can reach 8–12 Å. Such values for this mutual distance correspond to opposite locations in the cavity for the two species K^+ and H_2O. This feature is reproduced for most of the other water molecules in the cavity (not shown), indicating that solvation is a very dynamical process, *i.e.* there are permanent exchanges of water molecules in the solvation spheres.

4. Conclusion

We have shown that MD simulations complemented by arguments based on an electrostatic description of the protein can help to deepen our understanding of the role played by water molecules confined in the filter and the cavity of a KcsA pore. With regard to the formation of the K^+ ion sites and the dynamics of the ions, interesting features have also been obtained by comparing the behavior of water in the closed and open conformations of the pore. First, we demonstrated that water in the filter reinforces the potential wells' signature of the K^+ sites in the sequence KWKWK...K. Second, we observed that the water dipole orientations in the cavity are strongly correlated with the motions of the K_{cav} ion. This correlation nevertheless does not prevent water molecules from entering or exiting the cavity when the protein conformation changes (through opening or relaxation of the M_2 helices at the gate), and water diffusion proceeds by always keeping an optimal shell of oxygen atoms around the K^+ ions. A yet deeper insight to describe in a more explicit way the interactions between water, protein and K^+ ions could be provided (i) by the use of *ab initio* calculations and (ii) by considering the water diffusion over much longer times, which would require other numerical methods than MD, and would also allow the study of the variation of the number of water molecules in the cavity during the closing process.

References

1 N. Nandi, K. Bhattacharyya and B. Bagchi, *Chem. Rev.*, 2000, **100**, 2013.
2 S. Granick, *Science*, 1991, **253**, 1374.
3 M. S. P. Sansom, I. D. Kerr, J. Breed and R. Sankararamakrishnan, *Biophys. J.*, 1996, **70**, 693.
4 F. Merzel and J. C. Smith, *Proc. Natl. Acad. Sci. U. S. A.*, 2002, **99**, 5378.
5 M. S. P. Sansom, G. R. Smith, C. Adcock and P. C. Biggin, *Biophys. J.*, 1997, **73**, 2404.
6 S. W. Chiu, E. Jakobsson, S. Subramanian and J. A. McCammon, *Biophys. J.*, 1991, **60**, 273.
7 R. Lynden-Bell and J. C. Rasaiah, *J. Chem. Phys.*, 1996, **105**, 9266.
8 C. Y. Lee, J. A. McCammon and P. J. Rossky, *J. Chem. Phys.*, 1984, **80**, 4448.
9 R. Allen, S. Melchionna and J. P. Hansen, *Phys. Rev. Lett.*, 2002, **89**, 175502.

10 L. Zhang, H. T. Davis, D. M. Kroll and H. S. White, *J. Phys. Chem.*, 1995, **99**, 2878.
11 S. Senapati and A. Chandra, *J. Phys. Chem. B*, 2001, **105**, 5106.
12 M. S. P. Sansom, I. H. Shrivastava, J. N. Bright, J. Tate, C. Capener and P. Biggin, *Biochim. Biophys. Acta*, 2002, **1565**, 294.
13 L. Guidoni, V. Torre and P. Carloni, *Biochemistry*, 1999, **38**, 8599.
14 L. Guidoni and P. Carloni, *Biochim. Biophys. Acta*, 2002, **1563**, 1.
15 P. L. Luisi and B. Straub, *Reverse Micelles*, Plenum Press, New York, 1984.
16 D. Zhu, X. Wu and Z. A. Schelly, *J. Phys. Chem.*, 1992, **96**, 7121.
17 S. Das and K. Bhattacharyya, *J. Phys. Chem. A*, 1997, **101**, 3299.
18 S. Mashimo, S. Kuwabara, S. Yagihara and K. Higasi, *J. Phys. Chem.*, 1987, **91**, 6337.
19 D. Brown and J. Clarke, *J. Phys. Chem.*, 1988, **92**, 2881.
20 S. Vajda, R. Jimenez, S. Rosenthal, V. Fidler, G. R. Fleming and E. W. Castner Jr, *J. Chem. Soc., Faraday Trans.*, 1995, **91**, 867.
21 N. Nandi and B. Bagchi, *J. Phys. Chem.*, 1996, **100**, 13914.
22 P. A. Frey and W. W. Cleland, *Bioorg. Chem.*, 1998, **26**, 175.
23 W. W. Cleland, *Arch. Biochem. Biophys.*, 2000, **382**, 1.
24 M. E. Green, *J. Biomol. Struct. Dyn.*, 2002, **19**, 725.
25 D. A. Doyle, J. H. Cabral, R. A. Pfuetzner, A. Kuo, J. M. Gulbis, S. L. Cohen, B. T. Cahit and R. MacKinnon, *Science*, 1998, **280**, 69.
26 J. H. Morais-Cabral, Y. Zhou and R. MacKinnon, *Nature*, 2001, **414**, 37.
27 Y. Zhou, J. H. Morais-Cabral, A. Kaufman and R. MacKinnon, *Nature*, 2001, **414**, 43.
28 Y. Jiang, A. Lee, J. Chen, M. Cadene, B. T. Chait and R. MacKinnon, *Nature*, 2002, **417**, 515.
29 G. Chang, R. H. Spencer, A. T. Lee, M. T. Barclay and D. C. Rees, *Science*, 1998, **282**, 2220.
30 R. Dutzler, E. B. Campbell, M. Cadene, B. M. Chait and R. MacKinnon, *Nature*, 2002, **415**, 287.
31 N. Unwin, A. Miyazawa and Y. Fujiyoshi, *J. Mol. Biol.*, 2002, **319**, 1165.
32 A. Miyazawa, Y. Fujiyoshi and N. Unwin, *Nature*, 2003, **423**, 949.
33 B. Roux, S. Bernèche and W. Im, *Biochemistry*, 2000, **39**, 13295.
34 S. Bernèche and B. Roux, *Nature*, 2001, **414**, 73.
35 S. Bernèche and B. Roux, *Biophys. J.*, 2000, **78**, 2900.
36 C. Capener and M. P. Sansom, *J. Phys. Chem. B*, 2002, **106**, 4543.
37 I. H. Shrivastava and M. P. Sansom, *Biophys. J.*, 2000, **78**, 557.
38 P. C. Biggin, G. R. Smith, I. H. Shrivastava, S. Choe and M. P. Sansom, *Biochim. Biophys. Acta*, 2001, **1510**, 1.
39 P. C. Biggin and M. P. Sansom, *Biophys. J.*, 2002, **83**, 1867.
40 T. W. Allen, A. Bliznyuk, A. P. Rendell, S. Kuyucak and S. H. Chung, *J. Chem. Phys.*, 2000, **112**, 8191.
41 T. W. Allen and S. Chung, *Biochim. Biophys. Acta*, 2001, **1515**, 83.
42 L. Guidoni, V. Torre and P. Carloni, *FEBS Lett.*, 2000, **477**, 37.
43 V. Luzhkov and J. Åqvist, *Biochim. Biophys. Acta*, 2001, **1548**, 194.
44 F. M. Ashcroft, *Ion Channels and Disease*, Academic Press, San Diego, 2000.
45 B. Hille, *Ionic Channels of Excitable Membranes*, Sinauer Associates, Sunderland, MA, 2001.
46 G. Yellen, *Nature*, 2002, **419**, 35.
47 M. Compoint, P. Carloni, C. Ramseyer and C. Girardet, *Biochim. Biophys. Acta*, 2004, **1661**, 26.
48 M. Compoint, F. Picaud, C. Ramseyer and C. Girardet, *J. Chem. Phys.*, 2005, **122**, 045427.
49 M. Compoint, F. Picaud, C. Ramseyer and C. Girardet, *Chem. Phys. Lett.*, 2005, **407**, 199.
50 H. Woo, A. R. Dinner and B. Roux, *J. Chem. Phys.*, 2004, **121**, 6392.
51 Y. Jiang, A. Lee, J. Chen, M. Cadene, B. T. Chait and R. MacKinnon, *Nature*, 2002, **417**, 515.
52 Y. Jiang, A. Lee, J. Chen, V. Ruta, M. Cadene, B. T. Chait and R. MacKinnon, *Nature*, 2003, **423**, 33.
53 Q. X. Jiang, D. N. Wang and R. MacKinnon, *Nature*, 2004, **430**, 806.
54 E. Perozo, *Structure (London)*, 2002, **10**, 1027.
55 Y. S. Liu, P. Sompornpisut and E. Perozo, *Nat. Struct. Biol.*, 2001, **8**, 883.
56 E. Perozo, D. M. Cortes and L. G. Cuello, *Science*, 1999, **285**, 73.
57 S. H. Chung, T. W. Allen and S. Kuyucak, *Biophys. J.*, 2002, **82**, 628.
58 M. L. Connolly, *Science*, 1983, **221**, 709.
59 C. Miller, *Nature*, 2001, **414**, 23.
60 D. A. Case, D. A. Pearlman, J. W. Caldwell, T. E. Cheatham III, W. S. Ross, C. L. Simmerling, T. A. Darden, K. M. Merz, R. V. Stanton, A. L. Cheng, J. J. Vincent, M. Crowley, V. Tsui, R. J. Radmer, Y. Duan, J. Pitera, I. Massova, G. L. Seibel, U. C. Singh, P. K. Weiner and P. A. Kollman, *AMBER6*, University of California, San Francisco, 1999.
61 W. L. Jorgensen, J. Chandrasekhar and J. D. Madura, *J. Chem. Phys.*, 1983, **79**, 926.
62 H. J. C. Berendsen, J. P. M. Postma, W. F. Van Gunsteren, A. Di Nola and J. R. Haak, *J. Chem. Phys.*, 1984, **81**, 3684.
63 M. Compoint, C. Ramseyer and P. Huetz, *Chem. Phys. Lett.*, 2004, **395**, 510.
64 M. J. Frisch, G. W. Trucks, H. B. Schlegel, G. E. Scuseria, M. A. Robb, J. R. Cheeseman, J. A. Montgomery, Jr., T. Vreven, K. N. Kudin, J. C. Burant, J. M. Millam, S. S. Iyengar, J. Tomasi, V. Barone, B. Mennucci, M. Cossi, G. Scalmani, N. Rega, G. A. Petersson, H. Nakatsuji, M. Hada, M. Ehara, K. Toyota, R. Fukuda, J. Hasegawa, M. Ishida, T. Nakajima, Y. Honda, O. Kitao, H. Nakai, M. Klene, X. Li, J. E. Knox, H. P. Hratchian, J. B. Cross, C. Adamo, J. Jaramillo, R. Gomperts, R. E. Stratmann, O. Yazyev, A. J. Austin, R. Cammi, C. Pomelli, J. Ochterski, P. Y. Ayala, K. Morokuma, G. A. Voth, P. Salvador, J. J. Dannenberg, V. G. Zakrzewski, S. Dapprich, A. D. Daniels, M. C. Strain, O. Farkas, D. K. Malick, A. D. Rabuck, K. Raghavachari, J. B. Foresman, J. V. Ortiz, Q. Cui, A. G. Baboul, S. Clifford, J. Cioslowski, B. B. Stefanov, G. Liu, A. Liashenko, P. Piskorz, I. Komaromi, R. L. Martin, D. J. Fox, T. Keith, M. A. Al-Laham, C. Y. Peng, A. Nanayakkara, M. Challacombe, P. M. W. Gill, B. G. Johnson, W. Chen, M. W. Wong, C. Gonzalez and J. A. Pople, *GAUSSIAN 03 (Revision B.03)*, Gaussian, Inc., Pittsburgh PA, 2003, 41.
65 B. H. Besler, K. M. Merz Jr, and P. A. Kollman, *J. Comput. Chem.*, 1990, **11**, 431.
66 U. C. Singh and P. A. Kollman, *J. Comput. Chem.*, 1984, **5**, 129.